A&A, 692, A137 (2024)
https://doi.org/10.1051/0004-6361/202451737

Astronomy & Astrophysics

A tell-tale tracer for externally irradiated protoplanetary disks: Comparing the [C I] 8727 Å line and ALMA observations in proplyds★

M.-L. Aru[1,★★], K. Maucó[1], C. F. Manara[1], T. J. Haworth[2], N. Ballering[3], R. Boyden[3,4], J. Campbell-White[1], S. Facchini[5], G. P. Rosotti[5], A. Winter[11,12], A. Miotello[1], A. F. McLeod[6,7], M. Robberto[8,9], M. G. Petr-Gotzens[1], G. Ballabio[14], S. Vicente[10], M. Ansdell[13], and L. I. Cleeves[3]

[1] European Southern Observatory, Karl-Schwarzschild-Strasse 2, 85748 Garching bei München, Germany
[2] Astronomy Unit, School of Physics and Astronomy, Queen Mary University of London, London E1 4NS, UK
[3] Department of Astronomy, University of Virginia, Charlottesville, VA 22904, USA
[4] Space Science Institute, Boulder, CO 80301, USA
[5] Dipartimento di Fisica, Università degli Studi di Milano, Via Celoria 16, 20133 Milano, Italy
[6] Centre for Extragalactic Astronomy, Department of Physics, Durham University, South Road, Durham DH1 3LE, UK
[7] Department of Physics, Institute for Computational Cosmology, University of Durham, South Road, Durham DH1 3LE, UK
[8] Space Telescope Science Institute, 3700 San Martin Dr, Baltimore, MD 21218, USA
[9] Johns Hopkins University, 3400 N. Charles Street, Baltimore, MD 21218, USA
[10] Instituto de Astrofísica e Ciências do Espaco, Universidade de Lisboa, OAL, Tapada da Ajuda, 1349-018 Lisboa, Portugal
[11] Université Cote d'Azur, Observatoire de la Cote d'Azur, CNRS, Laboratoire Lagrange, 06300 Nice, France
[12] Universiíe Grenoble Alpes, CNRS, IPAG, 38000 Grenoble, France
[13] NASA Headquarters, 300 E Street SW, Washington, DC 20546, USA
[14] Imperial Astrophysics, Imperial College London, Blackett Laboratory, Prince Consort Road, London SW7 2AZ, UK

Received 31 July 2024 / Accepted 25 October 2024

ABSTRACT

The evolution of protoplanetary disks in regions with massive OB stars is influenced by externally driven winds that deplete the outer parts of these disks. The winds have previously been studied via forbidden oxygen emission lines, which also arise in isolated disks in low-mass star-forming regions (SFRs) with weak external UV fields in photoevaporative or magnetic (internal) disk winds. It is crucial to determine how to disentangle external winds from internal ones. Here, we report a proxy for unambiguously identifying externally driven winds with a forbidden line of neutral atomic carbon, [C I] 8727 Å. We compare for the first time the spatial location of the emission in the [O I] 5577 Å, [O I] 6300 Å, and [C I] 8727 Å lines traced by VLT/MUSE-NFM with the ALMA Band 7 continuum disk emission in a sample of 12 proplyds in the Orion Nebula Cluster (ONC). We confirm that the [O I] 5577 Å emission is co-spatial with the disk emission, whereas that of [O I] 6300 Å is emitted both on the disk surface and on the ionization front of the proplyds. We show for the first time that the [C I] 8727 Å line is also co-spatial with the disk surface in proplyds, as seen in the MUSE and ALMA data comparison. The peak emission is compatible with the stellar location in all cases, apart from one target with high relative inclination with respect to the ionizing radiation, where the peak emission is located at the disk edge in the direction of the ionizing radiation. To verify whether the [C I] 8727 Å line is detected in regions where external photoevaporation is not expected, we examined VLT/X-Shooter spectra for young stars in low-mass SFRs. Although the [O I] 5577 Å and 6300 Å lines are well detected in all these targets, the total detection rate is ≪10% in the case of the [C I] 8727 Å line. This number increases substantially to a ~40% detection rate in σ-Orionis, a region with higher UV radiation than in low-mass SFRs, but lower than in the ONC. The spatial location of the [C I] 8727 Å line emission and the lack of its detection in isolated disks in low-mass SFRs strongly suggest that this line is a tell-tale tracer of externally driven photoevaporative winds, which agrees with recent excitation models.

Key words. protoplanetary disks – stars: pre-main sequence – planetary nebulae: individual: Orion Nebula

1. Introduction

The evolution of protoplanetary disks is affected by their surrounding environment. In massive clusters, the UV radiation from OB stars heats the gas in nearby protoplanetary disks, and gives rise to externally driven photoevaporative wind. This wind depletes the disk outside-in, causing rapid mass loss and a shorter disk lifetime (see Winter & Haworth 2022 for a review).

Irradiated disks, typically called proplyds, have been studied best in the Orion Nebula Cluster (ONC), where they exhibit a teardrop shape with an ionization front as imaged with the *Hubble* Space Telescope (HST; e.g., O'Dell et al. 1993; Bally et al. 1998; Ricci et al. 2008), and more recently studied with the Multi-Unit Spectroscopic Explorer (MUSE) instrument in narrow-field mode (NFM) at the ESO Very Large Telescope (VLT, Kirwan et al. 2023; Haworth et al. 2023; Aru et al. 2024) and with JWST (Berné et al. 2023, 2024; Habart et al. 2024).

★ Based on observations collected at the European Southern Observatory under ESO programme 0104.C-0963(A), 106.218X.001, and 110.259E.001.
★★ Corresponding author; mariliis.aru@eso.org

While external photoevaporation of disks is unique to clusters with massive stars, such as the ONC, internal photoevaporative winds due to the high-energy radiation from the central star (e.g., Ercolano & Pascucci 2017) may be present in high-UV environments and in low-mass star-forming regions (SFRs) with weak external UV fields. Internal disk winds may also be magnetohydrodynamically driven (see Pascucci et al. 2023 for a review). The forbidden emission lines, such as [O I] 5577 Å and [O I] 6300 Å, are commonly observed in conjunction with both internally driven winds (e.g., Natta et al. 2014; Simon et al. 2016; Fang et al. 2018; Nisini et al. 2018; Banzatti et al. 2019; Gangi et al. 2023) and externally driven winds (e.g., Bally et al. 1998; Tsamis et al. 2013). In distant clusters, the proplyd morphology cannot be spatially resolved. Furthermore, there may be no ionization fronts in regions where the extreme-ultraviolet (EUV) field is attenuated or negligible (e.g., Haworth et al. 2023). These facts raise the question of how to identify external winds and how to disentangle them from internal ones. Ballabio et al. (2023) explore the line luminosity of [O I] 6300 Å as a diagnostic for external photoevaporation and predict it to undergo a dramatic increase above ~5000 G_0. However, it remains challenging to spectrally differentiate between internal and external winds without spatially resolving the system.

Here, we explore a proxy of externally driven winds, the near-IR forbidden line of neutral atomic carbon at 8727 Å covered by the MUSE-NFM data. Atomic carbon is predicted to be present in the upper layers of protoplanetary disks, where CO is dissociated by UV photons (e.g., Bruderer et al. 2012). Recently, [C I] 609 µm was detected in the isolated disk IM Lup with the Atacama Large Millimeter/submillimeter Array (ALMA) Band 8 observations, where it traces the disk atmosphere (Law et al. 2023), and in the irradiated disk d203-506 in the ONC, where it traces a photoevaporative wind (Goicoechea et al. 2024). Forbidden carbon lines at 8727 Å and 9850 Å were observed in emission in the ONC before the discovery of proplyds (Hippelein & Muench 1978 detected the two lines; Cosmovici et al. 1981 observed 8727 Å). Goicoechea et al. (2024) also report detecting the [C I] 9850 Å line in d203-506. Other carbon emission lines around ~1 µm were observed in the Orion Bar by Walmsley et al. (2000) and Peeters et al. (2024). Various permitted carbon emission lines in the same wavelength range were reported to be emitted in the inner regions of isolated disks by McClure (2019) and McClure et al. (2020), who did not detect near-IR carbon forbidden lines in these objects. More recently, [C I] 8727 Å was detected in two irradiated disks in the ONC (Haworth et al. 2023). This line, emitted at the 2.7 eV level in the transition $2p^2\ ^1D_2$, was theoretically studied by Escalante et al. (1991), as were two related forbidden lines at 9850 Å and 9823 Å. Escalante et al. (1991) reported that these lines originated from a combination of C^+ ions produced by photoionization in regions with a density greater than 10^5 cm^{-3} and radiation fields ~10^3–$10^6 G_0$, where G_0 is the interstellar field intensity. More recent models predict that the line is instead excited via far-ultraviolet (FUV) pumping and its intensity scales with G_0 (Goicoechea et al. 2024).

In this study, we build on these previous works to present strong evidence that the [C I] 8727 Å line can be used as a near-IR tracer for identifying externally photoevaporated disks by combining the information on the location of the emission in this line with that from the disk from 12 proplyds in the ONC observed with MUSE and with ALMA.

Table 1. Coordinates and projected separations of the sample of proplyds.

Proplyd	RA hh:mm:ss.s	Dec dd:mm:ss.s	d (UV source) (pc)
154–346	05:35:15.44	−05:23:45.55	0.068
167–325	05:35:16.72	−05:23:25.5	0.009
168–326	05:35:16.85	−05:23:26.22	0.012
170–249	05:35:16.96	−05:22:48.51	0.068
170–334	05:35:16.96	−05:23:33.6	0.028
170–337	05:35:16.97	−05:23:37.15	0.031
171–340	05:35:17.06	−05:23:39.77	0.037
173–236	05:35:17.34	−05:22:35.81	0.095
174–414	05:35:17.40	−05:24:14.5	0.106
177–341W	05:35:17.66	−05:23:41.00	0.049
203–504	05:35:20.26	−05:25:04.05	0.077 (θ^2 Ori A)
244–440	05:35:24.38	−05:24:39.74	0.06 (θ^2 Ori A)
			0.31 (θ^1 Ori C)

Notes. The information is from O'Dell & Wen (1994); Bally et al. (2000); Ricci et al. (2008); Mann et al. (2014). For the given projected separations, d, the UV source is θ^1 Ori C with the exception of 203–504 (irradiated by θ^2 Ori A) and 244–440.

2. Data and analysis

2.1. Observational data

We use data from the 12 proplyds showing prominent ionization fronts firstly presented by Aru et al. (2024). These objects were observed with the VLT/MUSE integral field spectrograph (Bacon et al. 2010). The coordinates of the targets are given in Table 1. MUSE was operated in NFM, which covers the wavelength range ~4750–9350 Å with a field of view of ~7.5″ × 7.5″. The observations were taken in three programs (Pr. ID 104.C-0963(A) and 106.218X.001, PI: C. F. Manara; Pr. ID 110.259E.001, PI: T. J. Haworth). We measured the angular resolution of the images in the full width at half maximum (FWHM) range ≈0.06–0.08″ at ~8760 Å in our observations. Details regarding the observation and the data reduction process are described in Haworth et al. (2023) for proplyd 203–504 and in Aru et al. (2024) for the rest of the sample.

In addition, we use the ALMA observations of six targets (168–326, 170–249, 170–337, 171–340, 173–236, and 177–341W) performed in Band 7 (0.86 mm) with an angular resolution of 0.09″. The ALMA Band 7 data trace thermal dust emission from the disk and are described in Eisner et al. (2018). Ballering et al. (2023) show that the Band 7 data do not trace the ionization front, which is instead traced by the Band 3 data as presented in their work. Lastly, we use the publicly available spectra taken with VLT/X-Shooter for the PENELLOPE Large Program (Manara et al. 2021) and those published by Maucó et al. (2023).

2.2. Data analysis

In the following analysis, we consider the [O I] lines at 5577 Å and 6300 Å and [C I] 8727 Å, observed with MUSE-NFM, and compare the location of the continuum-subtracted emission (see Aru et al. 2024 for details) with the locations of the ALMA disk continuum emission and the stellar continuum emission.

2.2.1. Alignment and spatial comparison

As MUSE-NFM is known to have an uncertain astrometric accuracy, it is necessary to align the MUSE cubes with the ALMA data before analyzing how the MUSE detections of [C I] 8727 Å, as well as [O I] 5577 Å and 6300 Å, emissions compare to the disk's dust observations of ALMA. The alignment was done by measuring relevant reference points in the MUSE and ALMA continuum images and shifting the coordinates of the ALMA image to align with MUSE.

In the case of 177–341W, we carried out the matching by using two background sources present in both the ALMA and the MUSE data. We refer readers to Appendix A for a more detailed discussion on this target and its alignment. For the remaining proplyds, we used a subcube of the MUSE observations nearly free of emission lines, showing the star continuum, at $\lambda \sim 674$–678 nm. We then aligned the location of the star, measured on the MUSE image, with the center of the disk in the ALMA continuum image. We considered the uncertainty on this alignment to be half the spatial size of the MUSE spaxels (0.0125″) for all proplyds except 168–326, 174–414, and 203–504, for which the spaxel size 0.025″ was used because the emission around the central star is more extended and therefore the location more uncertain.

In Fig. 1, the images of the ALMA Band 7 data are shown together with the line emission from MUSE, which is shown with contours representing 50%, 70%, and 90% of the peak intensity of the line emission. The proplyds are ordered starting from the smallest projected separation to θ^1 Ori C to the largest. The direction of the UV source is shown with an arrow. We report the inclinations of the disks, calculated from their deconvolved FWHM major and minor axes listed by Ballering et al. (2023) using the CASA task imfit on the ALMA data for proplyds 168–326 and 171–340.

We made a spatial comparison between the stellar emission location and the [O I] 5577 Å, 6300 Å, and [C I] 8727 Å line emission location to determine any spatial displacement. Figure 2 shows the MUSE stellar continuum emission and the contours of the emission lines in a similar way as Fig. 1. In Fig. 2, all 12 of the proplyds are shown, including those not observed with ALMA.

2.2.2. Radial cuts

In order to confirm that the line emission is spatially resolved and to analyze the shift of the emission lines in relation to the central star, we retrieved a radial cut for each proplyd in the MUSE emission line images. This was performed by calculating the emission along a 6″-long line centered at the coordinates of the central star and oriented toward the ionizing source θ^1 Ori C. The procedure is described in more detail in Aru et al. (2024). In the case of 177–341W, we instead centered the radial cut line at coordinates corresponding to the center of the disk as seen in the ALMA image. This is because the disk is highly inclined and the coordinates of the central star cannot be determined in the same way as for other proplyds. This target is discussed in more detail in Appendix A. Figures of radial cuts are described in Appendix B (available on Zenodo).

3. Results and discussion

Here, we describe the observed spatial location of the [O I] 5577 Å, 6300 Å, and [C I] 8727 Å lines observed with MUSE and how these compare with the disk emission traced by ALMA. Combining this information with an analysis of high-resolution spectra of young stars in low-mass SFRs, we show the potential of the [C I] line for tracing externally photoevaporated winds.

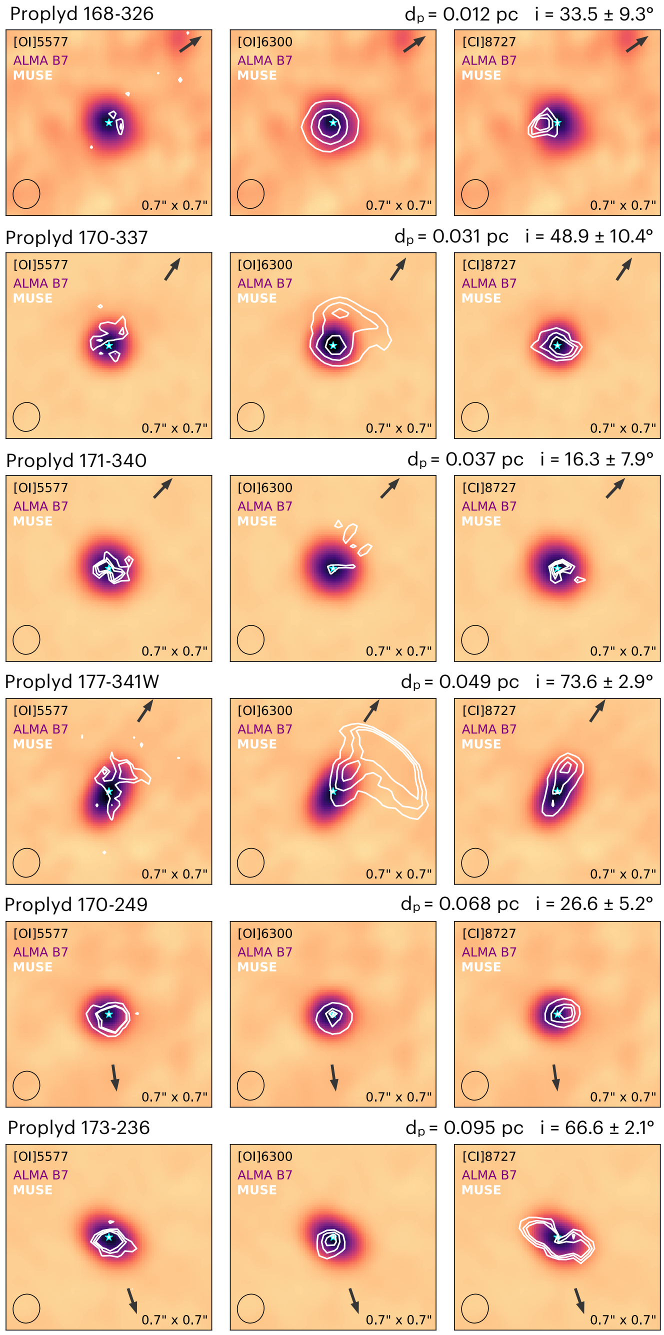

Fig. 1. ALMA Band 7 images of proplyds 168–326, 170–337, 171–340, 177–341W, 170–249, and 173–236 compared with the MUSE emission lines (contours) at 50%, 70%, and 90% of the peak intensity; the rows are ordered in increasing projected distance from θ^1 Ori C. The ALMA Band 7 data were originally published by Eisner et al. (2018); the values for inclination marked above the figures are from Ballering et al. (2023), except for 168–326 and 171–340 (Ballering et al., in prep.). The MUSE emission lines are shown in the top left corner, the beam size is indicated in the bottom left corner, and the size of each image in the bottom right corner. The direction of the UV source is shown with an arrow. The cyan star marks the star's estimated location.

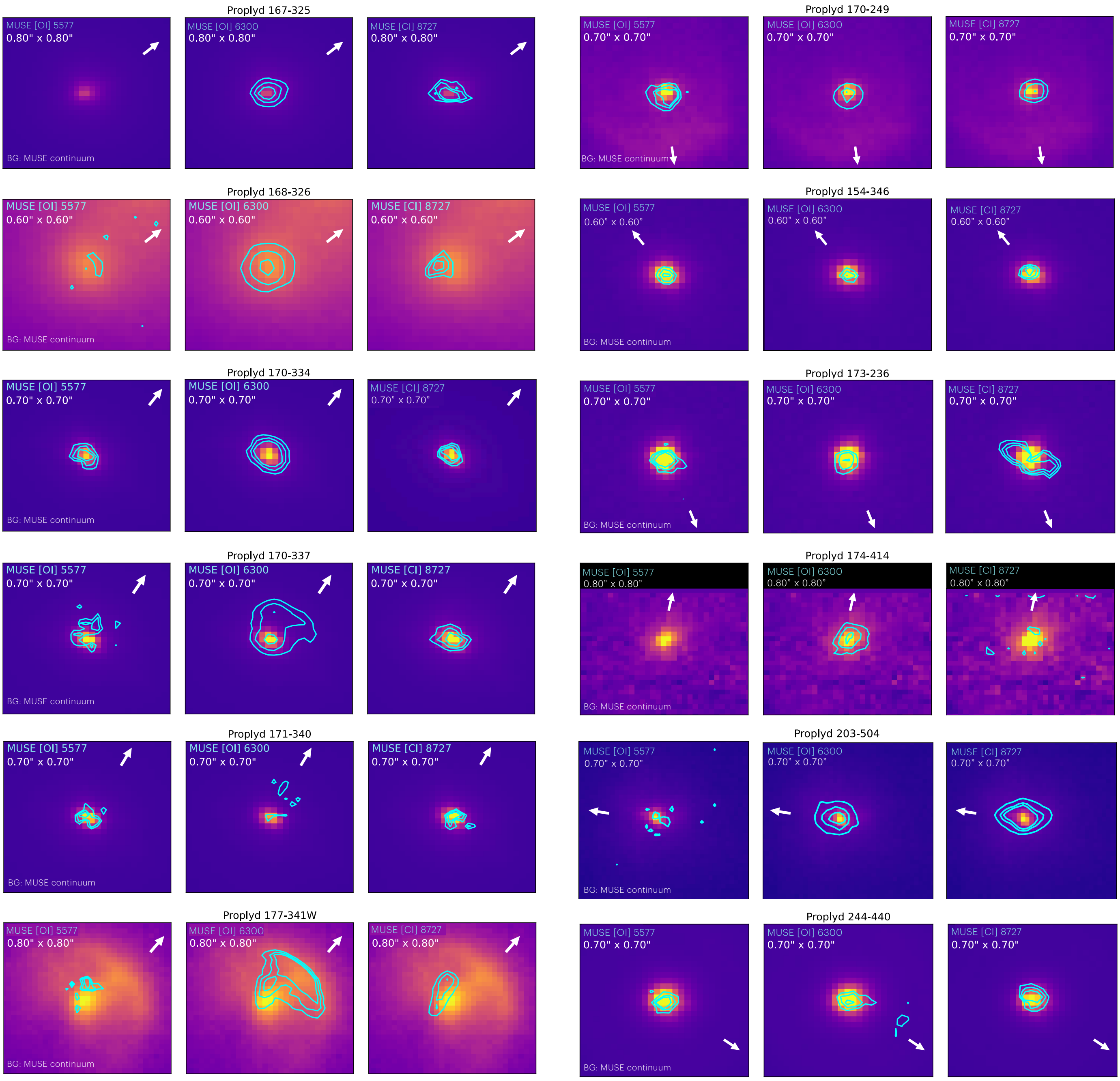

Fig. 2. Spatial comparison between MUSE stellar continuum (colormap) and MUSE emission lines (contours) for proplyds 154–346, 167–325, 168–326, 170–249, 170–334, 170–337, 171–340, 173–236, 174–414, 177–341W, 203–504, and 244–440. The emission line and the size of each image are shown in the top left corner. The contours represent 50%, 70%, and 90% of the peak intensity of the MUSE emission lines, except for the [C I] line of 174–414 for which only 90% is shown. The direction of the UV source is shown with an arrow.

3.1. [O I] 5577 Å, 6300 Å lines in proplyds

The [O I] 6300 Å line was detected in some of the proplyds in the ONC with HST (e.g., Bally et al. 1998), while [O I] 5577 Å was detected in proplyd 182–413 (also known as HST-10) with VLT/FLAMES (Tsamis et al. 2013). We detect both lines in all 12 proplyds of the sample. Here, we introduce a comparison between these oxygen emission lines and the ALMA disk continuum emission.

The location of the [O I] 5577 Å, 6300 Å emission lines is typically well aligned with the disk's dust emission from ALMA, as shown in Fig. 1. The emission of [O I] 5577 Å coincides with the disk, which is seen the most clearly, due to the lowest noise, in proplyds 170–249 and 173–236. We note that these are the two disks with the largest projected separation from the ionizing source in the combined MUSE-ALMA sample shown here. In the MUSE-MUSE comparison of Fig. 2, proplyds 170–334, 154–346, 203–504, and 244–440 also show the coincidence of the [O I] 5577 Å emission with the disk, under the assumption that the star is centered at the center of the disk. For 167–32 and 174–414, the MUSE moment 0 map is too noisy for [O I] 5577 Å contours to be shown.

Table 2. Coordinates and projected separations of the detected proplyds.

Proplyd (1)	Offset, [O I] (″) (2)	Offset, [C I] (″) (3)	i (deg) (4)	PA_d (deg) (5)	$PA_{d,\star}$ (deg) (6)
154–346	–0.003 ± 0.0125	0.015 ± 0.0125	...	...	38
167–325	–0.009 ± 0.0125	–0.021 ± 0.0125	...	...	126
168–326	–0.0150 ± 0.0250	–0.039 ± 0.0250	33.5 ± 9.3	31 ± 3	125
170–249	–0.0030 ± 0.0125	0.009 ± 0.0125	26.6 ± 5.2	68 ± 16	10
170–334	0.003 ± 0.0125	0.009 ± 0.0125	...	...	136
171–340	–0.0030 ± 0.0125	0.009 ± 0.0125	16.3 ± 7.9	41 ± 9	148
170–337	–0.0030 ± 0.0125	–0.003 ± 0.0125	48.9 ±10.4	85 ± 17	147
173–236	0.0030 ± 0.0125	–0.015 ± 0.0125	66.6 ± 2.1	60 ± 2	18
174–414	0.009 ± 0.0250	0.003 ± 0.0250	...	...	164
177–341W	0.0931 ± 0.0125	0.101 ± 0.0125	73.6 ± 2.9	152 ± 2	136
203–504	0.021 ± 0.0250	–0.015 ± 0.0250	...	...	75
244–440	0.009 ± 0.01	–0.033 ± 0.01	...	...	52

Notes. Column (1): Name of the proplyd. Column (2): Peak of [O I] 6300 Å emission measured from the location of the star in a radial cut; the sign indicates whether the peak is toward or in the opposite side from the UV source. Column (3): Similar to column (2) but for [C I] 8727 Å. Column (4): Inclination of the disk, calculated from the deconvolved FWHM major and minor axes of disks listed by Ballering et al. (2023) and Ballering et al. (in prep.), for proplyds 168–326 and 171–340. Column (5): Position angle of the deconvolved disk from ALMA data similarly to column (4). Column (6): Position angle between the disk and the UV source. As the inclination and PA_d are measured from ALMA data; the values are not available for the whole sample.

In a study of proplyd 182–413 (Tsamis et al. 2013), the line [O I] 5577 Å was found to peak at spaxels that coincide with the position of the disk and, therefore, align with our observations. We thus confirm that the [O I] 5577 Å emission originates on the disk surface.

The [O I] 5577 Å emission is not co-spatial with [O I] 6300 Å. The major difference between the two oxygen emission lines is that [O I] 5577 Å is only bound to the disk region and not emitted in the ionization front. The [O I] 6300 Å emission from the disk and the ionization front is connected in the contours for proplyds 170–337 and 177–341W; these locations match with the early observations described by Bally et al. (1998). Theoretical works have also predicted [O I] 6300 Å to trace multiple regions: the area near the disk surface, the photodissociation region, and the ionization front where oxygen is excited thermally due to collisions with H, H_2, and electrons (e.g., Störzer & Hollenbach 1998).

In Fig. 3 we show the displacement of the [O I] 6300 Å peak emission from the location of the star as a function of the UV radiation field. Values in the positive range of the y-axis mark a peak located in the direction of the UV source, and those in the negative range the opposite. These values are derived from the radial cuts (figures available on Zenodo), and given in Table 2. The values are compatible with no displacement within their uncertainties except for 177–341W, which has an inclined disk of $i = 73.6 \pm 2.9$ deg (Ballering et al. 2023).

To further investigate whether the offset of the emission peak is an effect related to the inclination of the disk relative to the UV source, we calculated the relative inclination of the disks using the spherical law of cosines: $\cos(\Delta i) = \cos(i_1)\cos(i_2) + \sin(i_1)\sin(i_2)\cos(\Omega_1 - \Omega_2)$, where Ω_1 is the position angle of the disk from ALMA, Ω_2 the position angle between the central star and the UV source, i_1 the disk inclination, and $i_2 = 90$ deg is the inclination we assume for the emission coming from the UV source in the plane of the sky. In Fig. 4, the displacements are shown as a function of the relative inclination. Proplyd 177–341W has the highest relative inclination, which could well explain the fact that the displacement arises from the disk's

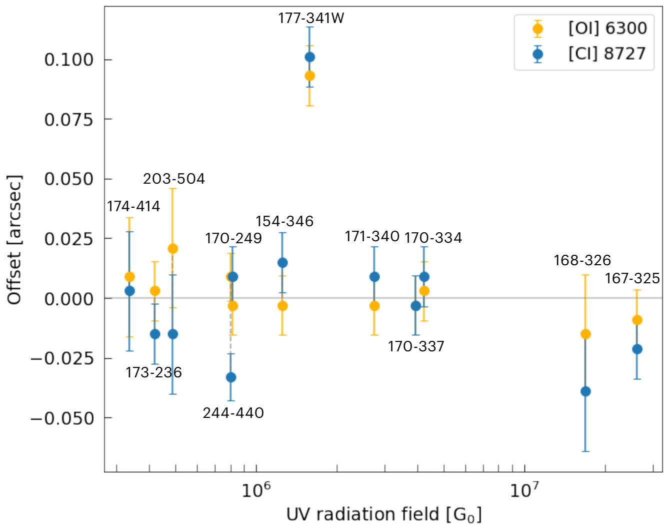

Fig. 3. Offsets between the intensity peaks of forbidden line emission and the location of the star versus the UV radiation field. The peak in the radial cut of [O I] 6300 Å is marked in orange, and blue points mark [C I] 8727 Å.

inclination relative to θ^1 Ori C. If the [O I] emission does mainly come from a wind on the surface of the disk, we would expect that this mainly arises from the edge of the disk on the side pointing toward the UV source θ^1 Ori C. In cases of low relative inclination, this effect is more difficult to see as the whole disk surface is irradiated, resulting in a more homogeneous emission. On the other hand, when the relative inclination is higher, then one side of the disk is more illuminated and the emission is stronger. This hypothesis needs confirmation on a larger sample of targets.

3.2. [C I] 8727 Å line in proplyds

The MUSE data provide the first detection of the [C I] 8727 Å emission line in proplyds (Haworth et al. 2023). Here, we present

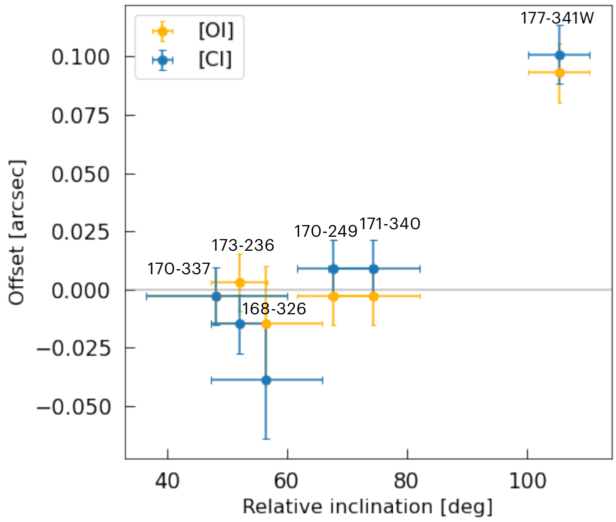

Fig. 4. Offsets between the intensity peaks of forbidden line emission and the location of the star, versus relative inclination. A relative inclination of 0 deg would correspond to a disk being irradiated face-on, and of about 90 deg to an edge-on configuration. The peak in the radial cut of [O I] 6300 Å is marked in yellow, and blue points mark the offset of [C I] 8727 Å.

for the first time a comparison between the [C I] 8727 Å emission and the ALMA dust emission, and the detection of this line in all 12 proplyds in our sample.

Firstly, the [C I] 8727 Å emission appears co-spatial with the ALMA disk emission. No contribution from the ionization front is present, and the line is emitted only from the disk surface and/or base of the externally photoevaporating wind. Compared to the contours of the [O I] λ5577, λ6300 lines, [C I] 8727 Å traces the disk shape more closely in the case of inclined disks 173–236 and 177–341W, as seen in Fig. 1. In the case of 173–236, the contours of [C I] 8727 Å follow an elliptical shape that coincides with the ALMA continuum image, rather than the circular contours of the [O I] 6300 Å emission line. The shape of the [C I] 8727 Å contours is also elliptical for 177–341W, whereas [O I] 5577 Å is not clear and the contours of [O I] 6300 Å are merged with the emission from the ionization front. For 170–337, [C I] 8727 Å also enables the disk to be located without noise or emission from the ionization front. Therefore, [C I] 8727 Å is a more accurate tracer of the disk surface and/or the base of the externally photoevaporating wind than the [O I] lines. Furthermore, the similarity between the gas radius and the dust continuum radius could potentially allow the [C I] 8727 Å emission line to be used for estimating the gas disk radius.

The [C I] 8727 Å emission is co-spatial with the MUSE stellar continuum emission for the rest of the proplyds in the sample (170–334, 174–414, 167–325, 154–346, 203–504, and 244–440). The stellar continuum, taken in an emission-line-free region of the MUSE cube between 8756–8764 Å, is shown in Fig. 2, together with the contours showing the location of the emission lines. When comparing the peak emission offset with the irradiation from the ionizing source on the targets (Fig. 3), including for the [C I] 8727 Å line, the biggest displacement is seen in 177–341W. For 177–341W, the [C I] 8727 Å emission peaks on the side of the disk facing toward the direction of the UV source. The offset between the center of the disk in the ALMA image and the peak of [C I] 8727 Å emission (MUSE) is shown as an outlier in Fig. 4, as the location of the star was assumed to be in the center of the disk. This peak implies that [C I] 8727 Å traces the surface of the disk and/or the base of the photoevaporative wind. Similarly to the discussion on the [O I] line offset, the largest offset in this case may be due to the high relative inclination of this disk with respect to θ^1 Ori C. The targets with lower relative inclinations show a more uniform emission on the disk surface. The lack of measurements for disk inclination and position angle for half of our sample hinders the possibility of further confirming that this is due to the relative inclination of the disks and the external UV radiation. An example of the proplyd morphology based on 177–341W as observed with MUSE is shown in Fig. 5.

Proplyd 168–326 is another outlier in Figs. 3 and 4, with the peak of [C I] 8727 Å facing away from θ^1 Ori C. This proplyd has the second smallest projected separation (d_p=0.012 pc) from the UV source among the 12 targets. However, the contours of nearby proplyd 167–325 (d_p=0.009 pc) coincide with the location of the central star, as seen in Fig. 2. Therefore, it is unclear whether the displacement of [C I] 8727 Å could be explained by the small projected separation. We also note that, for this target, the offset is still compatible with zero, and therefore it is harder to conclude any statistically sound difference.

Finally, we note that 244–440 also has a peak offset of the [C I] 8727 Å line slightly larger than zero and in the opposite direction of the ionizing radiation (Fig. 3). We note, however, that this is a peculiar target, possibly irradiated by two UV sources (O'Dell et al. 2017). The properties of this proplyd are discussed in more detail in Aru et al. (2024) and it will be the subject of future studies.

3.3. The [C I] 8727 Å line as a tracer of externally photoevaporated disks

The spatial location of the [C I] 8727 Å emission strongly suggests that this line originates on the disk surface and/or the base of the externally photoevaporating wind. It is interesting to verify whether this line also traces disk winds in low-ionization environments, where external photoevaporation is not at play. This is the case for the [O I] lines, routinely detected in isolated disks in low-mass SFRs and interpreted in those environments as tracers of internal – photoevaporative or magnetohydrodynamic (MHD) – winds (Pascucci et al. 2023, for a review).

To verify whether the [C I] 8727 Å line is also typical in disks in low-mass SFRs, where external photoevaporation is not expected, we examined 74 VLT/X-Shooter spectra from the PENELLOPE Large Program (Manara et al. 2021, regions such as ϵ Cha, Lupus, and Taurus) and 45 VLT/X-Shooter spectra from the study of σ-Orionis by Maucó et al. (2023). The [O I] 5577 Å line is detected in 68% of the targets, and the [O I] 6300 Å line in 88% of the targets in the PENELLOPE sample (Campbell-White, in prep.). In contrast, only one target shows a clear detection of the [C I] 8727 Å line in the PENELLOPE sample, with seven additional tentative detections, for a total of a $\ll$10% detection rate. This number increases substantially to a ~40% detection rate in σ-Orionis, a region with higher UV radiation than low-mass SFRs, but lower than the ONC. It is to be expected that a good fraction of the targets in this region are indeed experiencing external photoevaporation winds. Lastly, we detect this line in all 12 proplyds in the ONC observed with MUSE/NFM. The lack of detections in isolated disks is consistent with McClure (2019) and McClure et al. (2020), who did not

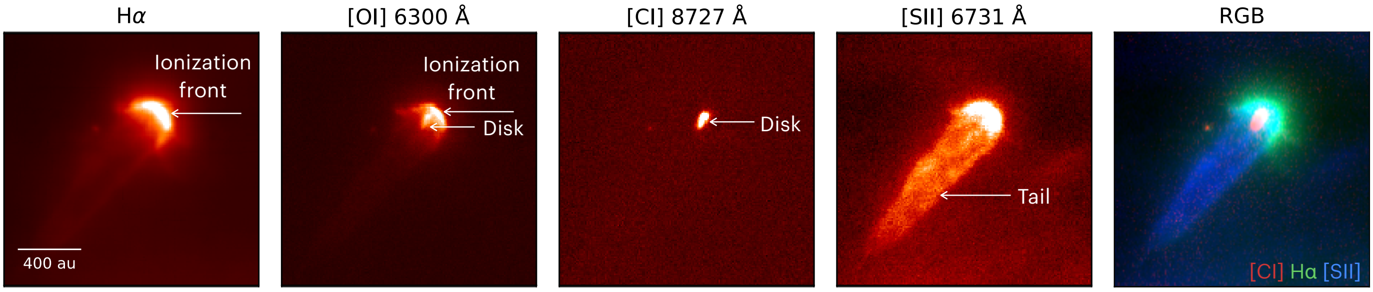

Fig. 5. Continuum-subtracted, single-line integrated flux images and an RGB image of proplyd 177–341W. The panels show which parts of the system are visible in given emission lines.

detect IR carbon forbidden lines in the innermost regions of isolated disks, where instead they detected several permitted carbon lines. In the same disks, previous works had detected forbidden lines of [O I] in the vast majority of the targets (Natta et al. 2014; Nisini et al. 2018).

This notable difference in detection rates between the [O I] optical lines and the [C I] 8727 Å lines in disks in low-mass SFRs strongly points to the fact that this line is emitted in highly externally irradiated environments. This is in agreement with the results found by Escalante et al. (1991), who pointed to high external UV flux in cluster environments, such as the one experienced by proplyds, for this line to be emitted. We note that they considered the 10^3–10^6 G_0 FUV field range, and that the FUV field of our targets expands this range into lower values, with 10^2 G_0 in σ-Orionis and a higher range for the proplyds closest to θ^1 Ori C in the ONC (167–325 and 168–326; 10^7 G_0). Our results are in even greater agreement with the FUV-pumping excitation models of Goicoechea et al. (2024). Their models also predict that the intensity of the IR carbon lines scales with G_0. This dependence should be explored in future works. As expected from these models, the emission of [C I] 8727 Å is confined to the disk and/or base of the externally photoevaporating wind, and does not appear on the ionization front, in agreement with the fact that these are not recombination lines. The detection rate, together with the coincidence of the emission with the disk surface, strongly suggest that the [C I] 8727 Å line is emitted in an externally photoevaporated wind and does not suffer from confusion with line emission due to internal processes, such as in the cases of the [O I] lines, known tracers of internal processes (e.g., Ercolano & Pascucci 2017), and external winds (e.g, Ballabio et al. 2023).

4. Conclusions

In this work, we compared the spatial location traced by VLT/MUSE-NFM of the emission in the [O I] 6300 Å and [O I] 5577 Å lines, as well as in the [C I] 8727 Å line, with the ALMA Band 7 continuum disk emission in a sample of 12 proplyds in the ONC. We confirm that the [O I] emission is co-spatial with the disk emission for the [O I] 5577 Å line, whereas that of [O I] 6300 Å is emitted both on the disk surface and on the ionization front of the proplyds. At the same time, we show for the first time that [C I] 8727 Å is also co-spatial with the disk surface in a proplyd, as seen in the MUSE and ALMA data comparison. The peak emission is compatible with the stellar location in all cases, apart from one target with high relative inclination with respect to the UV radiation, where the peak emission is located at the disk edge in the direction of the UV radiation.

We have presented the [C I] 8727 Å emission line in the 12 proplyds that were observed with MUSE in NFM, with a detection rate of 100%. In contrast, this line has a much lower detection rate in other SFRs, and this rate decreases to become compatible with zero detections in the nearby low-mass SFRs. This result strongly supports the recent excitation models of neutral carbon in externally irradiated disks proposed by Goicoechea et al. (2024). On the other hand, [O I] lines at 5577 Å and 6300 Å are common in low-mass SFRs, as they are also related to internal disk winds, and this contamination makes them a less direct tracer of externally driven winds.

Our results strongly suggest that:

- The [C I] 8727 Å line traces the base of the externally photoevaporated wind, can act as a key tracer of the wind, and is ideal for distinguishing winds in disks that are not externally photoevaporated, such as in low-mass SFRs;
- This emission can be particularly valuable for identifying external irradiation when there is no ionization front or proplyd morphology visible (as in the case of d203-506; Haworth et al. 2023);
- As the dust continuum radius is very similar to the gas radius, the [C I] line could be a potential tracer of the gas disk radius (and by extension, the gas-disk size distribution) in irradiated environments, which is set to be explored in future works.

Our work highlights the strength of using the [C I] 8727 Å line as a proxy for tracing external photoevaporation. With VLT/MUSE, it may be systematically easier to detect large samples of externally photoevaporated gas disks in massive clusters, and to study the global spatial extents of the dust versus gas at large samples in combination with ALMA.

Future studies should aim to study the kinematics of this line by using spectral resolutions inaccessible with MUSE-NFM, to confirm that this line is tracing a slow wind, as expected from externally photoevaporated winds (Ballabio et al. 2023). Additional surveys with ALMA should be carried out to measure the disk inclination and position angles, as well as the disk sizes, in a larger number of proplyds, which are to then be combined with the MUSE data to further decipher their physical conditions.

Data availability

Additional data for this article are available at `https://zenodo.org/doi/10.5281/zenodo.14002504`.

Acknowledgements. We thank the anonymous referee for detailed comments and useful suggestions, which improved our work. MLA, KM, CFM, and JCW are funded by the European Union (ERC, WANDA, 101039452). GPR is funded by the European Union (ERC, DiscEvol, 101039651) and by the Fondazione

Cariplo, grant no. 2022-1217. SF is funded by the European Union (ERC, UNVEIL, 101076613), and acknowledges financial contribution from PRIN-MUR 2022YP5ACE. TJH acknowledges funding from a Royal Society Dorothy Hodgkin Fellowship and UKRI guaranteed funding for a Horizon Europe ERC consolidator grant (EP/Y024710/1). GB is supported by the European Research Council (ERC) under the European Union's Horizon 2020 research and innovation programme (Grant agreement No. 853022, PEVAP). Views and opinions expressed are however those of the author(s) only and do not necessarily reflect those of the European Union or the European Research Council Executive Agency. Neither the European Union nor the granting authority can be held responsible for them. This paper makes use of the following ALMA data: ADS/JAO.ALMA #2015.1.00534.S. ALMA is a partnership of ESO (representing its member states), NSF (USA) and NINS (Japan), together with NRC (Canada), NSTC and ASIAA (Taiwan), and KASI (Republic of Korea), in cooperation with the Republic of Chile. The Joint ALMA Observatory is operated by ESO, AUI/NRAO and NAOJ.

References

Aru, M. L., Maucó, K., Manara, C. F., et al. 2024, A&A, 687, A93
Bacon, R., Accardo, M., Adjali, L., et al. 2010, SPIE Conf. Ser., 7735, 773508
Ballabio, G., Haworth, T. J., & Henney, W. J. 2023, MNRAS, 518, 5563
Ballering, N. P., Cleeves, L. I., Haworth, T. J., et al. 2023, ApJ, 954, 127
Bally, J., Sutherland, R. S., Devine, D., & Johnstone, D. 1998, AJ, 116, 293
Bally, J., O'Dell, C. R., & McCaughrean, M. J. 2000, AJ, 119, 2919
Banzatti, A., Pascucci, I., Edwards, S., et al. 2019, ApJ, 870, 76
Berné, O., Martin-Drumel, M.-A., Schroetter, I., et al. 2023, Nature, 621, 56
Berné, O., Habart, E., Peeters, E., et al. 2024, Science, 383, 988
Bruderer, S., van Dishoeck, E. F., Doty, S. D., & Herczeg, G. J. 2012, A&A, 541, A91
Cosmovici, C. B., Strafella, F., & Iijima, T. 1981, A&A, 101, 397
Eisner, J. A., Arce, H. G., Ballering, N. P., et al. 2018, ApJ, 860, 77
Ercolano, B., & Pascucci, I. 2017, Roy. Soc. Open Sci., 4, 170114
Escalante, V., Sternberg, A., & Dalgarno, A. 1991, ApJ, 375, 630
Fang, M., Pascucci, I., Edwards, S., et al. 2018, ApJ, 868, 28
Gangi, M., Nisini, B., Manara, C. F., et al. 2023, A&A, 675, A153
Goicoechea, J. R., Le Bourlot, J., Black, J. H., et al. 2024, A&A, 689, L4
Habart, E., Peeters, E., Berné, O., et al. 2024, A&A, 685, A73
Haworth, T. J., Reiter, M., O'Dell, C. R., et al. 2023, MNRAS, 525, 4129
Hippelein, H., & Muench, G. 1978, A&A, 68, L7
Kirwan, A., Manara, C. F., Whelan, E. T., et al. 2023, A&A, 673, A166
Law, C. J., Alarcón, F., Cleeves, L. I., Öberg, K. I., & Paneque-Carreño, T. 2023, ApJ, 959, L27
Manara, C. F., Frasca, A., Venuti, L., et al. 2021, A&A, 650, A196
Mann, R. K., Di Francesco, J., Johnstone, D., et al. 2014, ApJ, 784, 82
Maucó, K., Manara, C. F., Ansdell, M., et al. 2023, A&A, 680, C1
McClure, M. K. 2019, A&A, 632, A32
McClure, M. K., Dominik, C., & Kama, M. 2020, A&A, 642, L15
Natta, A., Testi, L., Alcalá, J. M., et al. 2014, A&A, 569, A5
Nisini, B., Antoniucci, S., Alcalá, J. M., et al. 2018, A&A, 609, A87
O'Dell, C. R., & Wen, Z. 1994, ApJ, 436, 194
O'Dell, C. R., Wen, Z., & Hu, X. 1993, ApJ, 410, 696
O'Dell, C. R., Kollatschny, W., & Ferland, G. J. 2017, ApJ, 837, 151
Pascucci, I., Cabrit, S., Edwards, S., et al. 2023, in Astronomical Society of the Pacific Conference Series, 534, Protostars and Planets VII, eds. S. Inutsuka, Y. Aikawa, T. Muto, K. Tomida, & M. Tamura, 567
Peeters, E., Habart, E., Berné, O., et al. 2024, A&A, 685, A74
Ricci, L., Robberto, M., & Soderblom, D. R. 2008, AJ, 136, 2136
Simon, M. N., Pascucci, I., Edwards, S., et al. 2016, ApJ, 831, 169
Störzer, H., & Hollenbach, D. 1998, ApJ, 502, L71
Tsamis, Y. G., Flores-Fajardo, N., Henney, W. J., Walsh, J. R., & Mesa-Delgado, A. 2013, MNRAS, 430, 3406
Villenave, M., Ménard, F., Dent, W. R. F., et al. 2020, A&A, 642, A164
Walmsley, C. M., Natta, A., Oliva, E., & Testi, L. 2000, A&A, 364, 301
Winter, A. J., & Haworth, T. J. 2022, Eur. Phys. J. Plus, 137, 1132

Appendix A: The case of proplyd 177-341W

With Fig. A.1, we investigate the location of the disk (observed in ALMA band 7) with respect to the subcube nearly free of emission lines (left-most panel) and the jet as seen in the emission line [Fe II] 8892 Å observed with MUSE (middle panel). We also show the [C I] emission observed with MUSE as overlaid on the moment 0 map showing the jet (right-most panel).

The jet pinpoints to the center of the disk and therefore the location of the star, further indicating that the peak of the emission in the left-most panel is misaligned from the true location of the star. The case of 177-341W is similar to the scattered light images of highly inclined disks studied by Villenave et al. (2020).

Appendix B: Additional figures

The figures available on Zenodo show: (1) the [C I] line at 8727 Å in the 12 proplyds is shown. The spectra were extracted from continuum subtracted cubes of wavelength range 8660–8760 Å on the emission, by using a circular aperture of 0.1"; (2) the radial cuts of 12 proplyds for the MUSE stellar continuum, and the moment 0 maps of [O I] 5577 Å and [C I] 8727 Å emission. These radial profiles were taken in the direction of the UV source, and allowed us to measure the peak of the emission lines with respect to the location of the star; (3) the spectra of eight tentative detections of the [C I] 8727 line, out of 74 targets observed with VLT/X-Shooter. The clearest detection is seen in the case of AA Tau.

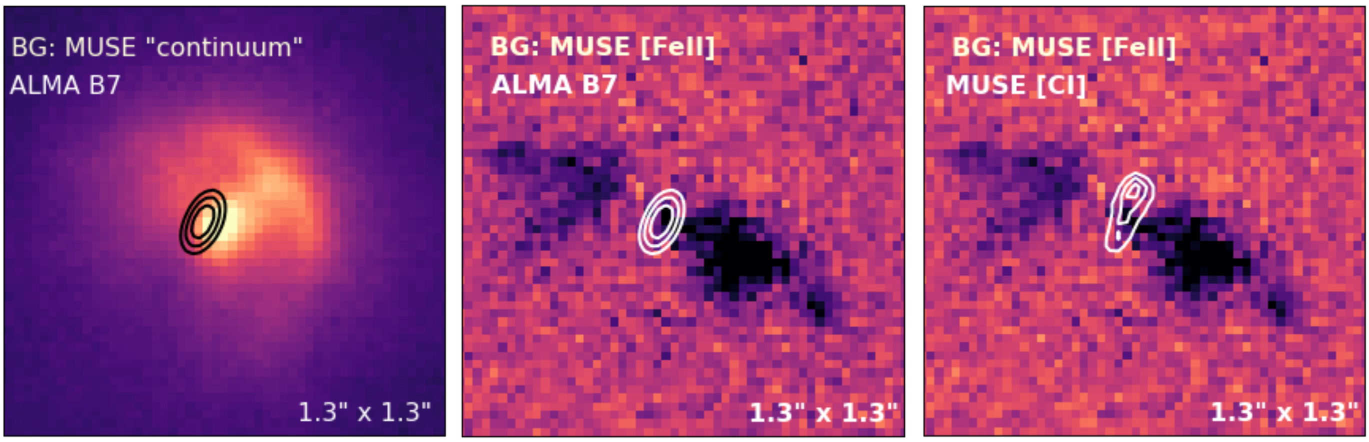

Fig. A.1. Proplyd 177-341W shown for three cases: 1) the stellar continuum emission in the background, overlaid with the contours of ALMA Band 7 data; 2) [Fe II] 8892 Å (MUSE) in the background, overlaid with the contours of ALMA Band 7 data; 3) [Fe II] 8892 Å (MUSE) in the background, overlaid with the contours of [C I] 8727 (MUSE).